inventions

MDPI

Article

Developments in the Use of $H_{infinity}$ Control and μ-Analysis for Reducing Vibration in Intelligent Structures

Amalia Moutsopoulou [1], Georgios E. Stavroulakis [2], Markos Petousis [1,*], Anastasios Pouliezos [2] and Nectarios Vidakis [1]

[1] Department of Mechanical Engineering, Hellenic Mediterranean University Estavromenos, GR-71410 Heraklion, Greece; amalia@hmu.gr (A.M.); vidakis@hmu.gr (N.V.)
[2] Department of Production Engineering and Management, Technical University of Crete, GR-73100 Chania, Greece; gestavroulakis@tuc.gr (G.E.S.); tasos@dpem.tuc.gr (A.P.)
* Correspondence: markospetousis@hmu.gr; Tel.: +30-28-1037-9227

Abstract: During the past few years, there has been a notable surge of interest in the field of smart structures. An intelligent structure is one that automatically responds to mechanical disturbances by minimizing oscillations after intelligently detecting them. In this study, a smart design that contains integrated actuators and sensors that can dampen oscillations is shown. A finite element analysis is used in conjunction with the application of dynamic loads such as wind force. The dynamic-loading-induced vibration of the intelligent piezoelectric structure is aimed to be mitigated using a μ-controller. The controller's robustness against uncertainties in the parameters to address vibration-related concerns is showcased. This article offers a thorough depiction of the benefits stemming from μ-analysis and active vibration control in the behavior of intelligent structures. The gradual surmounting of these challenges is attributed to the increasing affordability and enhanced capability of electronic components used for control implementation. The advancement of μ-analysis and robust control for vibration reduction in intelligent structures is amply demonstrated in this study.

Keywords: smart structures; reduced vibration; μ-analysis; robust control; controller; μ-synthesis

Citation: Moutsopoulou, A.; Stavroulakis, G.E.; Petousis, M.; Pouliezos, A.; Vidakis, N. Developments in the Use of $H_{infinity}$ Control and μ-Analysis for Reducing Vibration in Intelligent Structures. *Inventions* **2023**, *8*, 119. https://doi.org/10.3390/inventions8050119

Academic Editor: Wei Min Huang

Received: 24 August 2023
Revised: 19 September 2023
Accepted: 21 September 2023
Published: 25 September 2023

1. Introduction

Since structures must now be lighter, more flexible, and stronger because of changes in structural design, light structures have increasingly been employed in a variety of engineering applications in recent years [1–4]. In many situations where it is preferable to avoid adding extra stiffeners or dampers to a structure, the employment of active control vibration suppression methods for extremely lightweight constructions is a significant aim. Additionally, active approaches are better suited when the parameters of the regulated system or the disturbance to be canceled change over time [5–7]. Any structure that sags under a load can be considered to be a distributed parameter system and flexible structure. Active controllable smart electro/magneto materials open up novel avenues for the design of exceptionally accurate and efficient devices, structures, structural electronics, and mechatronic systems [8–10]. As is obvious, the contribution of control is very important in structural engineering. Many researchers have dealt with the application of smart materials in the sciences. There is a lot of research about such types of applications. Some famous and recent publications are below [11–13].

In this work, innovations are presented for the damping of structural oscillations and the introduction of uncertainty into simulation models through the mass and stiffness matrices. The suppression of oscillations is achieved even for very large changes in the initial matrices of the model, which is a great innovation in engineering. By amalgamating smart materials, sensors/actuators, control electronics, computers, and artificial intelligence, traditional mechatronic devices or systems undergo significant enhancement, giving

rise to an entirely new era of fully integrated smart structures. Owing to their lightweight nature and capacity to connect strain with electric fields, piezoelectric sensors, and actuators find extensive applications across various practical domains, notably including smart constructions. Piezoelectric sensors and actuators may be easily attached to vibrating structures to regulate structural vibrations [12–14]. In our paper, we use piezoelectric sensors and actuators in engineering structures. The nominal system, or the beam with known elastic, piezoelectric, and viscous characteristics, is first analyzed to better understand the optimum control issue [14,15]. Control systems are often applied to structures to optimize their response [16–18].

The resilience of the control in the presence of flaws is also addressed, which is a more practical query. Both the noise from measurements and the fact that systems are affected by disturbances such as wind power are taken into consideration. An approximate version of the genuine mathematical pattern is employed in the design. Additionally, two control rules, $H_{infinity,}$ and μ-analysis, are created for the composite plate to reduce vibrations [19–21]. Utilizing the provided measurements (displacement) and control inputs, the control objective revolves around upholding the equilibrium of the plate. This involves countering external disturbances, noise, and model imperfections to sustain zero displacements and rotations.

2. Materials and Methods

2.1. Equation of Motion of the Smart Structure

The equation of the beam for mechanical and electrical loading is given by the Euler–Bernoulli assumption [22]. In this work, the Euler–Bernoulli model is used because the simulation is performed using a thin beam. The piezoelectrics have very small dimensions and are integrated into the beam. In our future paper, we will deal with thick plates and more complex constructions, taking into account the Timoshenko model. The earliest and most straightforward classical theory for beam bending is the Euler–Bernoulli beam theory. It is applied in customary manual beam deflection calculations (Figure 1). It is predicted that the beam's cross-section is always parallel to the neutral axis (even after deformation). Shear forces are not taken into consideration; only the bending moment is used to compute the deflection. The intelligent structure we employ is made of pzt materials, which provide a bending moment. The Pzt materials are fitted and embedded in the beam.

$$EI\frac{\partial^4 y(t,x)}{\partial x^4} + \rho A\frac{\partial^2 y(t,x)}{\partial t^2} = f_m(t,x) + f_e(t,x) \quad (1)$$

where A is the area of the cross-section of the beam, ρ is the density of the beam, I is the moment of inertia of the beam, and E is Young's modulus of the beam.

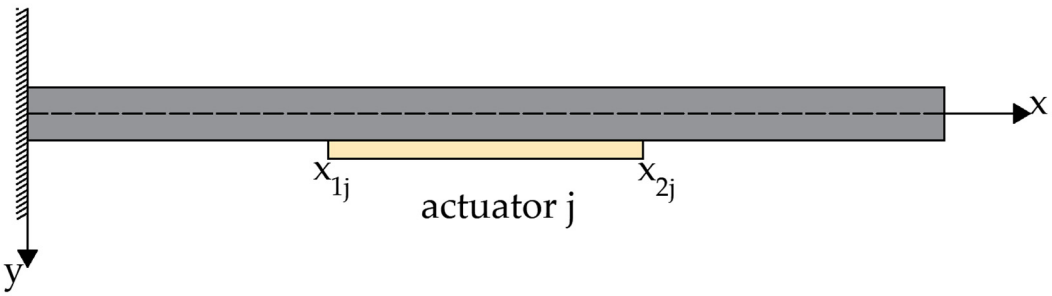

Figure 1. Piezoelectric section j embedded at the beam.

In Figure 2, we can see the smart beam with an embedded piezoelectric actuator, which produces mechanical force as an output when it has electrical force as an input [19–22]. The electric force $f_e(t,x)$ due to the piezoelectric activator is given by,

$$f_e(t,x) = \frac{\partial^2 M_{px}(t,x)}{\partial x^2} \quad (2)$$

where M_{px} represents torsion due to the piezoelectric actuator.

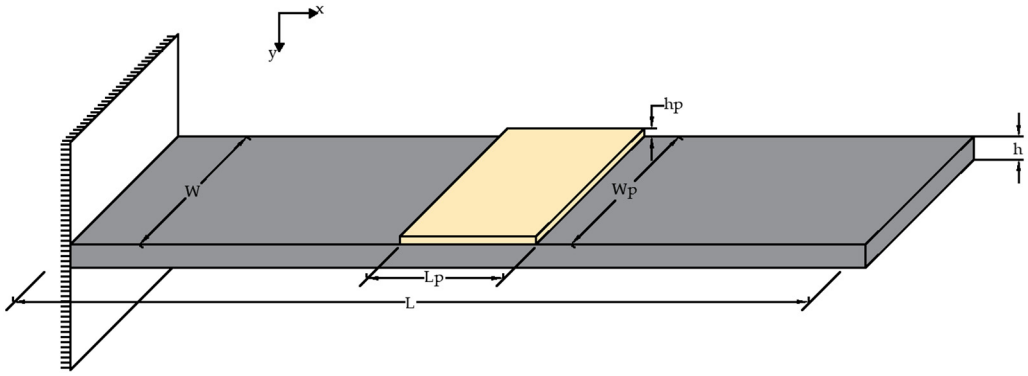

Figure 2. Beam with an attached piezoelectric patch.

The shape function H is used to represent the displacement of the piezoelectric patch on the beam. The torsion M_{px} from the pzt is given by,

$$M_{px}(t,x) = C_0 e_{pe}(t)\left[H(r-r_{1j}) - H(r-r_{2j})\right]u_j(t) \tag{3}$$

where,

$$C_0 = EI{\cdot}K_f \tag{4}$$

$$K_f = \frac{12EE_p h h_p (2h+h_p)}{16E^2h^4 + EE_p\left(32h^3h_p + 24h^2h_p^2 + 8hh_p^3\right) + E_p^2h_p^4} \tag{5}$$

In Table 1 and Figure 3, we take our smart structure parameters.
The mechanical tension $e_{pe}(t)$ due to the piezoelectric patch is given by,

$$e_{pe}(t) = \frac{d_{31}}{h_p}u_j(t) \tag{6}$$

Thus, Equation (3) can be written as,

$$M_{px}(t,x) = C_p\left[H(r-r_{1j}) - H(r-r_{2j})\right]u_j(t) \tag{7}$$

where,

$$C_p = EIK_f\frac{d_{31}}{h_p}$$

After partial production running at Equation (2), using (3), the electric force is given by,

$$f_e(t,x) = C_p u_{aj}(t)\left[\delta'(r-r_{1j}) - \delta'(r-r_{2j})\right] \tag{8}$$

where,

$$\int_{-\infty}^{\infty}\delta^{(n)}(t-\theta)\varphi(t) = (-1)^n\varphi^{(n)}(\theta)$$

From (1), using (8), the equation of the smart beam during vertical dynamical disturbance $q_0(t)$ and the electrical dynamical force due to the piezoelectric patch are given by,

$$EI\frac{\partial^4 y(t,x)}{\partial x^4} + \rho A = q_0(t) + C_p u_j(t)[\delta'(r-r_{1j}) - \delta'(r-r_{2j})] \tag{9}$$

For a similar piezoelectric (Figure 3), Equation (9) becomes:

$$EI\frac{\partial^4 y(t,x)}{\partial x^4} + \rho A\frac{\partial^2 y(t,x)}{\partial t^2} = q_0(t) + C_p u_j(t)\sum_{i=1}^{j}\left[\delta'(r-r_{1j}) - \delta'(r-r_{2j})\right] \tag{10}$$

Table 1. Smart beam characteristics.

Parameters	Values
L, for beam length	1.20 m
W, for beam width	0.004 m
W_p, pzt width	0.004 m
h, for beam thickness	0.096 m
h_p, piezoelectric thickness	0.0002 m
ρ, for beam density	1700 kg/m^3
E, for Young's modulus of the beam	1.6×10^{11} N/m^2
E_p, Young modulus of pzt	6.3×10^{10} N/m^2
bs, ba, for Pzt thickness	0.002 m
d_{31} the Piezoelectric constant	250×10^{-12} m/V

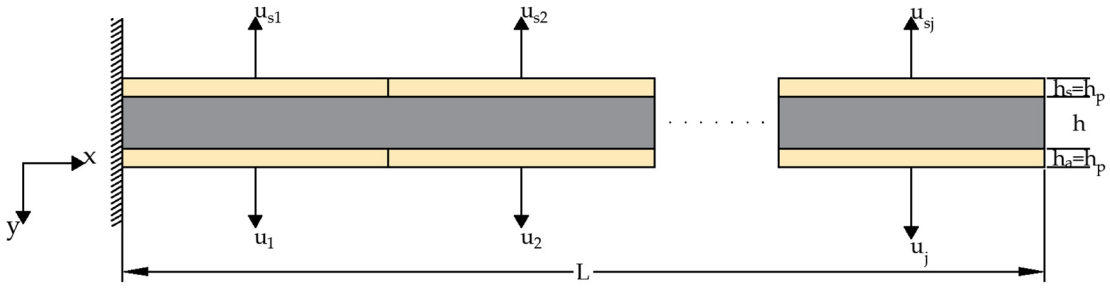

Figure 3. Smart beam with embedded piezoelectric actuators and sensors.

2.2. Modelling

This work deals with the reduction in oscillations using piezoelectric and advanced control techniques. The case of piezoelectric placement is taken. In Figure 4, the actuators are placed across the beam [23].

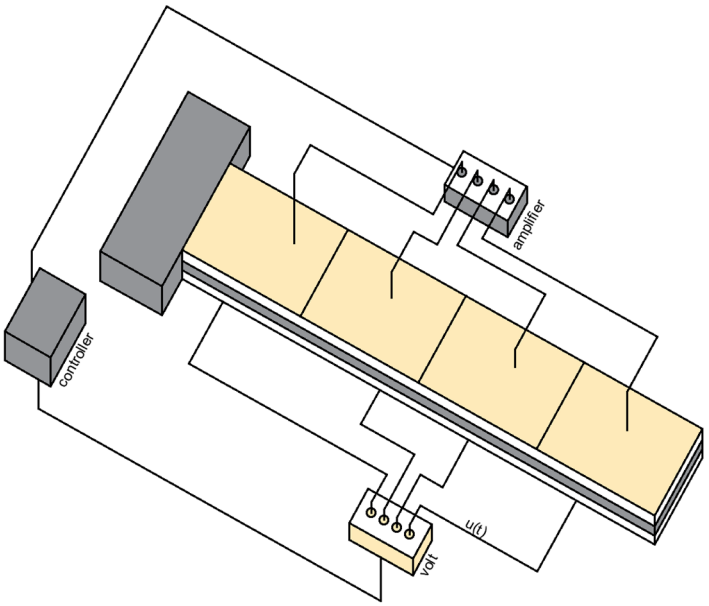

Figure 4. Schematic formulation of intelligent structure.

The system's dynamic characteristics are described as follows,

$$M\ddot{q}(t) + D\dot{q}(t) + Kq(t) = f_m(t) + f_e(t) \quad (11)$$

Here, let us break down the provided information:

f_m: This represents the overall external loading mechanical vector.
K: This stands for the global stiffness matrix.
M: This represents the global mass matrix.
D: This is the viscous damping matrix.
f_e: This denotes the global control force vector arising from electromechanical coupling effects.
Rotations w_i and transversal deflections ψ_i: These components constitute the independent variable q(t).

So, in essence, the equation relates various components in the context of a smart beam. It involves the global external loading mechanical vector (fm), the global mass matrix (M), the global stiffness matrix (K), the viscous damping matrix (D), and the global control force vector (fe) resulting from electromechanical coupling. The independent variable q(t) consists of rotations (w_i) and transverse deflections (ψ_i):

$$q(t) = \begin{bmatrix} w_1 \\ \psi_1 \\ \vdots \\ w_n \\ \psi_n \end{bmatrix} \tag{12}$$

With 'n' representing, in the analysis, the finite elements number employed, the subsequent procedure involves transforming these data into a state space control representation, following the conventional methodology.

$$\begin{aligned} x(t) &= \begin{bmatrix} q(t) \\ \dot{q}(t) \end{bmatrix} \\ \dot{x}(t) &= \begin{bmatrix} 0_{2n\times n} \\ M^{-1}(f_m(t) + f_e(t) \end{bmatrix} + \begin{bmatrix} \dot{q}(t) \\ -M^{-1}D\dot{q}(t) - M^{-1}Kq(t) \end{bmatrix} \\ &= \begin{bmatrix} 0_{2n\times n} \\ M^{-1}(f_m + f_e)(t) \end{bmatrix} + \begin{bmatrix} 0_{2n\times 2n} & I_{2n\times 2n} \\ -M^{-1}K & -M^{-1}D \end{bmatrix} \begin{bmatrix} q(t) \\ \dot{q}(t) \end{bmatrix} \\ &= \begin{bmatrix} 0_{2n\times n} \\ M^{-1}f_m(t) \end{bmatrix} + \begin{bmatrix} 0_{2n\times n} \\ M^{-1}f_e(t) \end{bmatrix} + \begin{bmatrix} 0_{2n\times 2n} & I_{2n\times 2n} \\ -M^{-1}K & -M^{-1}D \end{bmatrix} \begin{bmatrix} q(t) \\ \dot{q}(t) \end{bmatrix} \end{aligned} \tag{13}$$

Additionally, we define $f_e(t) = F_e \times u(t)$ as, where (of size $2n \times n$) is the piezoelectric force resulting from applying a unit input to the corresponding actuator [15,19–21],

$$F_e = \begin{bmatrix} 0 & 0 & 0 & 0 \\ cp & -cp & 0 & 0 \\ 0 & 0 & 0 & 0 \\ 0 & cp & -cp & 0 \\ 0 & 0 & 0 & 0 \\ 0 & 0 & cp & -cp \\ 0 & 0 & 0 & 0 \\ 0 & 0 & 0 & cp \end{bmatrix} \tag{14}$$

and u represents the voltages applied to the actuators. Finally, the disturbance vector is $d(t) = f_m(t)$. Then,

$$\begin{aligned} \dot{x}(t) = \begin{bmatrix} 0_{2n\times 2n} & I_{2n\times 2n} \\ -M^{-1}K & -M^{-1}D \end{bmatrix} x(t) + \begin{bmatrix} 0_{2n\times n} \\ M^{-1}F_e^* \end{bmatrix} u(t) + \begin{bmatrix} 0_{2n\times 2n} \\ M^{-1} \end{bmatrix} d(t) \\ = Ax(t) + Bu(t) + Gd(t) \\ = Ax(t) + [BG] \begin{bmatrix} u(t) \\ d(t) \end{bmatrix} \\ = Ax(t) + \widetilde{B}\widetilde{u}(t) \end{aligned} \tag{15}$$

With the output equation (displacements are just measured), we can improve this.

$$y(t) = [x1(t)\ x3(t) \ldots xn - 1(t)]T = C\ x(t)$$

The parameters of our system are shown in Table 1 and Figures 3 and 5.

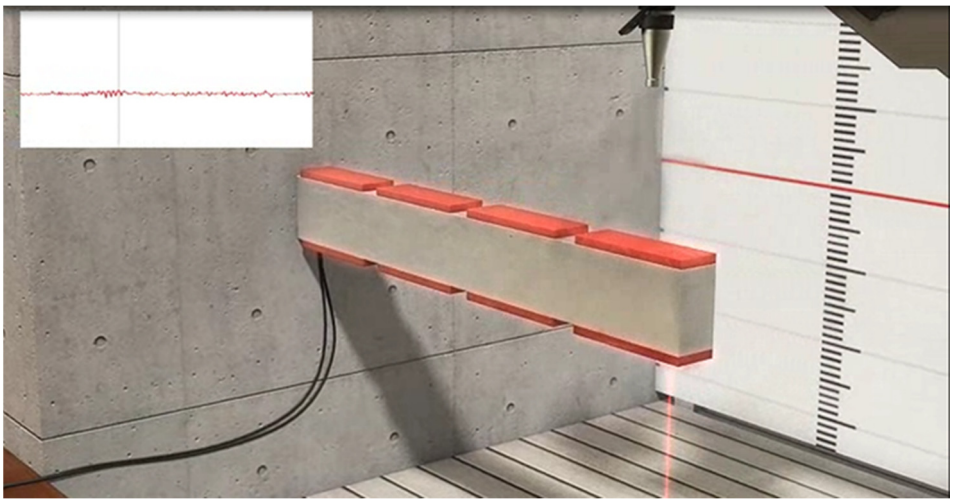

Figure 5. Intelligent structure.

3. Results

3.1. Robustness Issues

H∞ ($H_{infinity}$) control offers a significant advantage by effectively addressing the most pronounced effects of the unexpected noise and disturbances present in a system. Furthermore, it enables the design of an $H_{infinity}$ controller that showcases robustness against a predetermined degree of modeling inaccuracies. Unfortunately, as will be shown in the examples that follow [24,25], this last alternative is not always implementable.

The planned $H_{infinity}$ controller's resistance to modeling mistakes will be examined in the sections that follow. The presentation will also encompass an effort to construct a μ-controller, followed by a thorough comparison between the two approaches. For all the simulation scenarios, procedures from MATLAB's Robust Control Toolbox will be employed, specifically:

1. For uncertain elements, bw1 = ureal('bw1', 1, 'Percentage', 25)
   which implements a real uncertain element 'bw1' of a nominal value 1 and variation ±25%, i.e., bw1 ranges from 0.75 to 1.25.
2. To compute the limits on the structured singular value, bounds = mussv(Spqf, Bl);
   where Spqf is an frd object of the system (i.e., a frequency response output) and Bl defines the uncertainty type.
3. To calculate a μ-controller, K = dksyn(qbeam1_u, m, r);
   where qbeam1_u defines the uncertain system and m and r are the numbers of inputs/outputs of the system. In this case, the uncertain system is created through the iconnect structure, since it is more versatile than sysic.

The numerical models utilized in all the simulations are realized using three distinct approaches:

1. Through Equation (16),

$$\begin{gathered} M = M_0 + M_0(I + m_p\delta_M) \\ M_0 \text{ is the initial Mass Matrix} \\ K_0 \text{ is the initial Stiffness Matrix:} \\ K = K_0 + K_0(I + k_p\delta_K) \\ D = D_0 + 0.0005[K_0k_pI_{2n\times 2n}\delta_K + M_0m_pI_{2n\times 2n}\delta_M] \end{gathered} \tag{16}$$

followed by the subsequent assessment of matrix N for specific values of k_p and m_p.

2. Through the utilization of MATLAB's "uncertain element object", which is essential to the D-K robust synthesis algorithm.
3. Via Simulink implementation (Figure 6a,b)

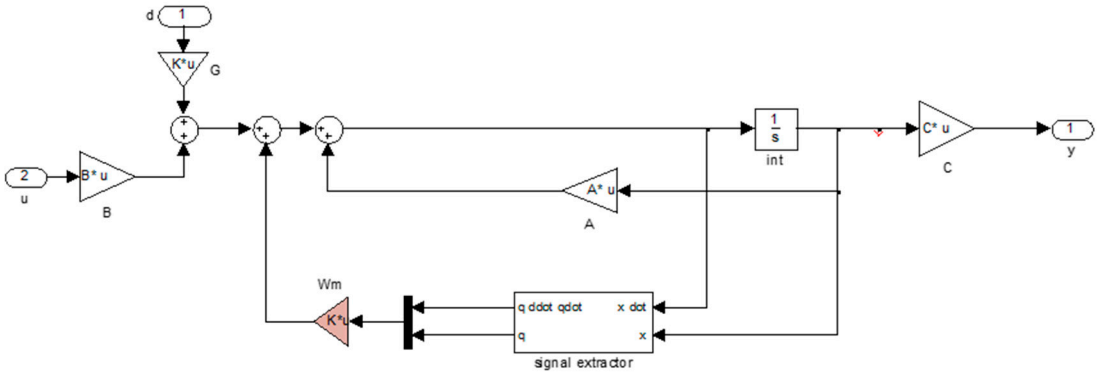

(**a**)

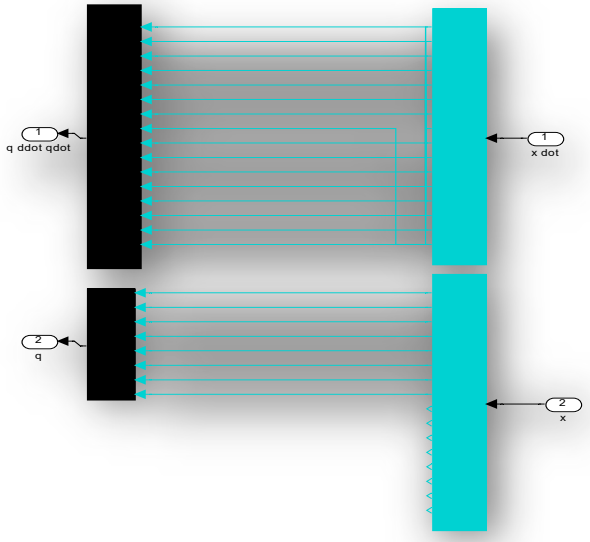

(**b**)

Figure 6. Simulink diagram of (**a**) the uncertain plant and (**b**) the signal extractor.

3.2. Robust Analysis

A robust analysis is performed by utilizing the relations:

$$\sup_{\omega \in \mathbb{R}} \mu_{\Delta}(N_{11}(j\omega)) < 1 \tag{17}$$

(for robust stability), and,

$$\sup_{\omega \in \mathbb{R}} \mu_{\Delta_a}(N(j\omega)) < 1 \tag{18}$$

for robust performance [26–28].

The initial disturbance, in all the subsequent simulations, consists of two components: the first being a dynamic wind force (depicted in Figure 7), and the second being a mechanical load of 10 N applied at the free end. The robust analysis was then carried out for the H∞ controller obtained, spanning the designated values of m_p and k_p.

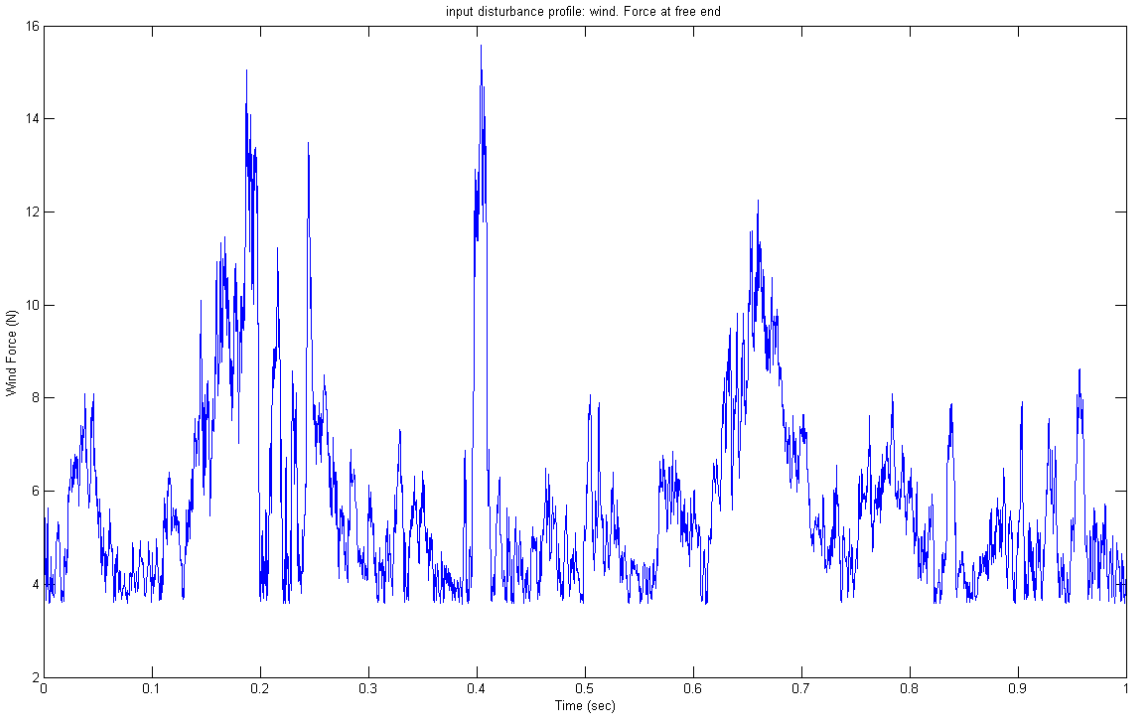

Figure 7. The dynamical wind force at the free end of the smart structures.

For the case where $m_p = 0$ and $k_p = 0.9$, which translates to a $\pm 90\%$ deviation from the nominal stiffness matrix K, the response of the displacement is illustrated in Figure 8 when subjected to the dynamic input. Figure 9 depicts the boundaries of these values. The system retains its stability and robust performance, evidenced by the fact that the upper limits of both values consistently remain below 1 across all the pertinent frequencies.

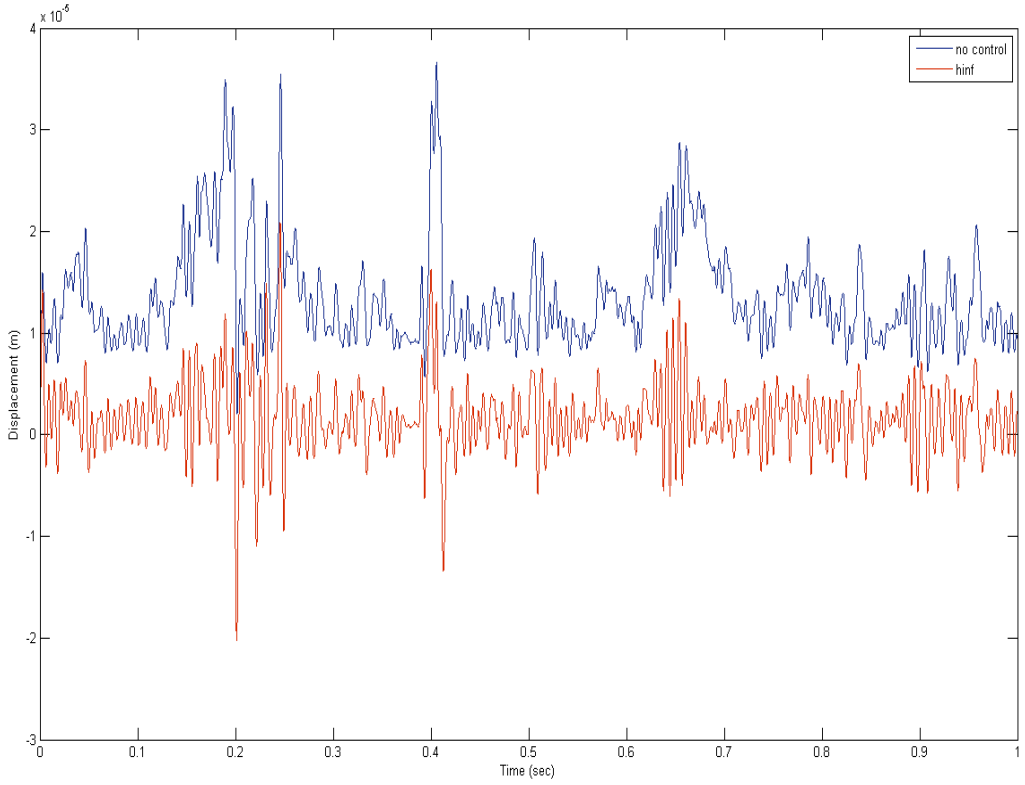

Figure 8. Displacement response, of the free end for $m_p = 0$ and $k_p = 0.9$.

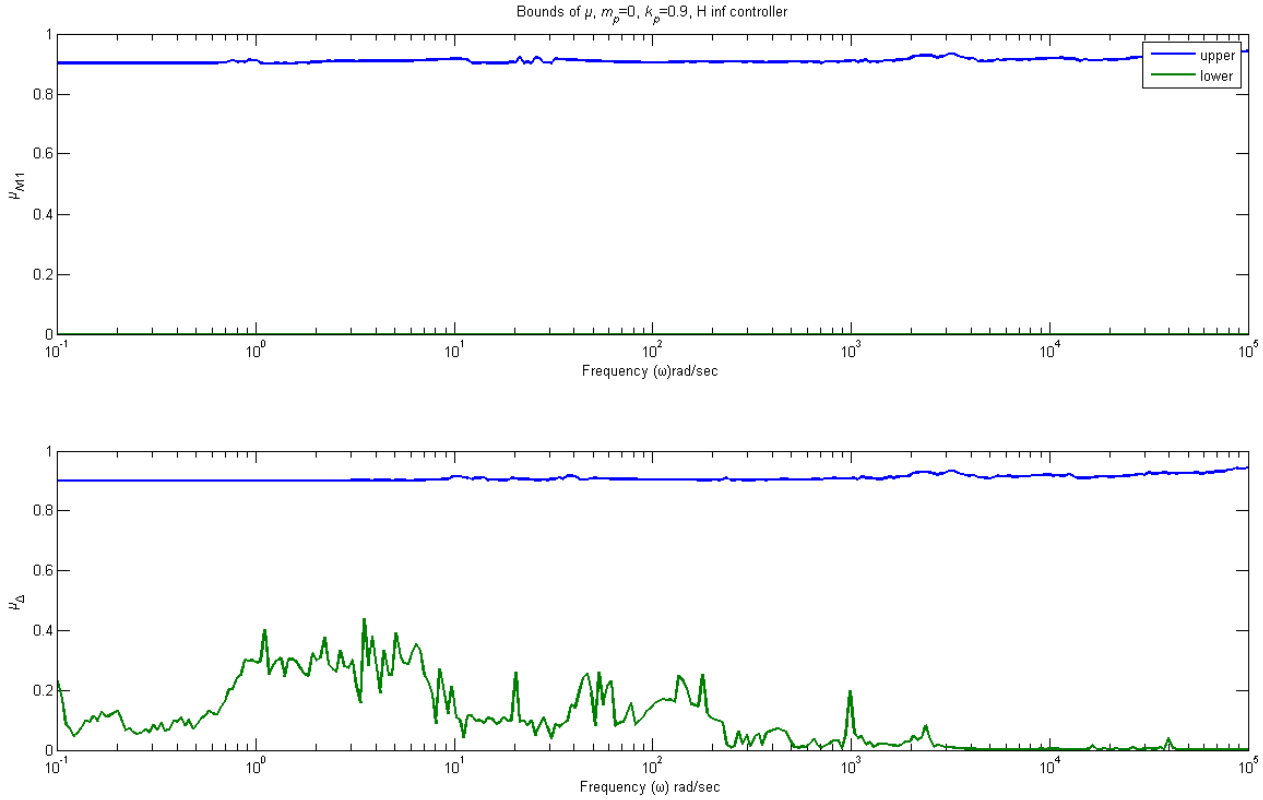

Figure 9. μ-bounds of the H∞ controller corresponding to $m_p = 0$ and $k_p = 0.9$.

Figure 10 provides further support for this assertion, showcasing the applied voltage and displacement of the free end amidst a notable level of uncertainty. For the same system, comparing this to the open-loop response, the nominal controller demonstrates a commendable performance. Figure 10 shows the voltages for the last four nodes of the vector; the blue color is for the last node, which means the free end of the beam (one actuator), the red is for the seventh node (two actuators), the green is for the sixth node (three actuators), and the light blue is for the fifth node (four actuators). At all the nodes, the voltages are much less than 500 V, which is the limit of piezoelectric patches.

For the case where $m_p = 0.9$ and $k_p = 0$: this represents a notable ±90% deviation from the nominal mass matrix M. Figure 11 visually presents the limits for these values, demonstrating that the system maintains its stability and functions efficiently. Remarkably, the upper limits of both values persistently remain below 1 across the pertinent frequencies. This assertion gains further support from Figure 12, which showcases the displacement response of the free end to the first dynamic input, in addition to the applied voltage. Comparing this to the open-loop response of the same plant, it is evident that the nominal controller performs well. Figure 12 shows the results for mp = 0.9, which is (m_p) a numerical vector that translates to a ±90% deviation from the nominal stiffness matrix M, i.e., as obtained from the relation change in mass by 1.9 from the initial value. Please see Equation (16).

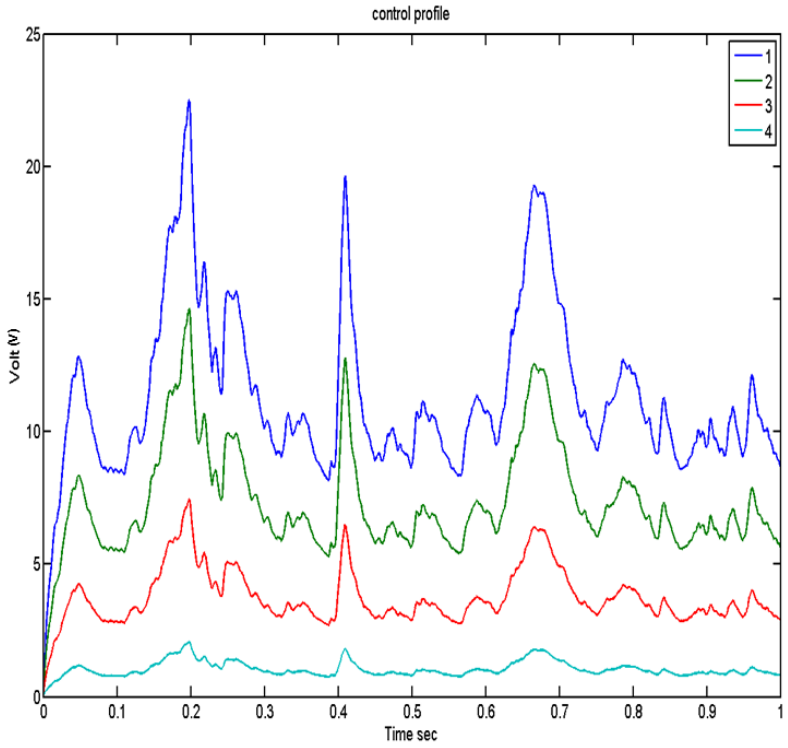

Figure 10. The response of displacement and control at the free end for the H∞ controller with $m_p = 0$ and $k_p = 0.9$ (at the extreme values). No 1 (blue graph) is the free end, no 2 (green graph) is the previous to last node, no 3 (red graph) is the one before that, and no 4 (light blue graph) is the middle node.

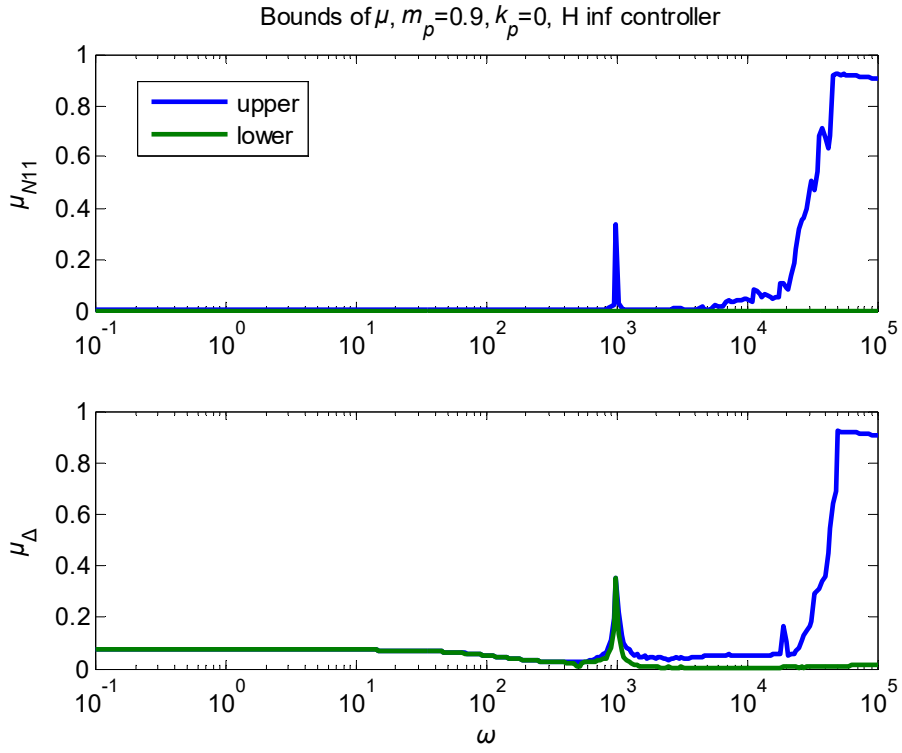

Figure 11. μ-bounds of the $H_{infinity}$ controller for $m_p = 0.9$ and $k_p = 0$.

For the scenario where $m_p = 0.9$ and $k_p = 0.9$: this equates to a substantial ±90% variation from the nominal values of both the mass matrix M and stiffness matrix K. Figure 12 shows the results for $m_p = 0.9$, where mp is a numerical vector, which translates

to a ±90% deviation from the nominal mass matrix M = 1.9M_0 (Equation (16)), i.e., as obtained from the relation change in mass by 1.9 from the initial value.

Figure 13 illustrates the limits of these values. Clearly, the system maintains its stability and demonstrates robust behavior, given that the upper bounds of both values consistently stay below 1 for all the pertinent frequencies.

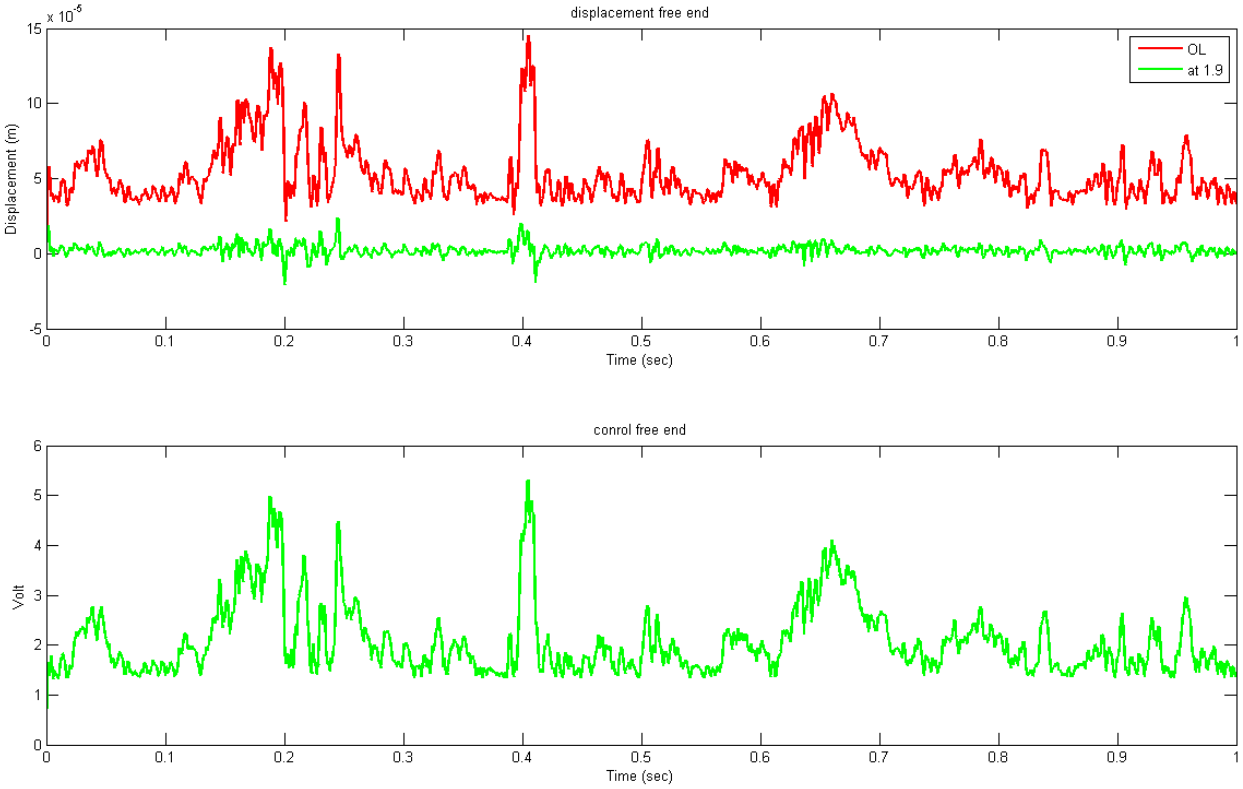

Figure 12. The displacement and control responses at the free end for the H∞ controller with m_p = 0.9, k_p = 0. OL is the open loop (without control) and the green line is the closed loop with control when M = 1.9 M_0.

By employing the structured uncertainty of the real plant, the μ-analysis can increase the precision of the singular value function of the closed-loop system. The so-called D-K iteration, which may be employed in the μ-synthesis to improve the controller, takes the structured singular value function into account. The weighting factor and controller are developed using this procedure in repeated rounds. This method still works, even if the joint optimization or D-K iteration are not convex, and global convergence is not guaranteed. The goal of this study is to demonstrate a $H_{infinity}$-based control design strategy that offers reliable stability and minimal performance. A number of nominal performances and strong stability parameters will be supplied, since they are crucial for the controller. The purpose of this work is to present a $H_{infinity}$-based control design approach that provides a nominal performance and dependable stability. Since it is crucial for the controller design that these two types of criteria be stated, a number of nominal performances and robust stability characteristics will be provided. However, this problem is more difficult given that an identification process produces the nominal model of the inverted pendulum. For the selection of the strong stability and nominal performance criteria, a variety of design options are presented. Despite meeting the necessary high stability criteria, to ensure a nominal and dependable performance, the developed controller employs D-K iteration in the synthesis.

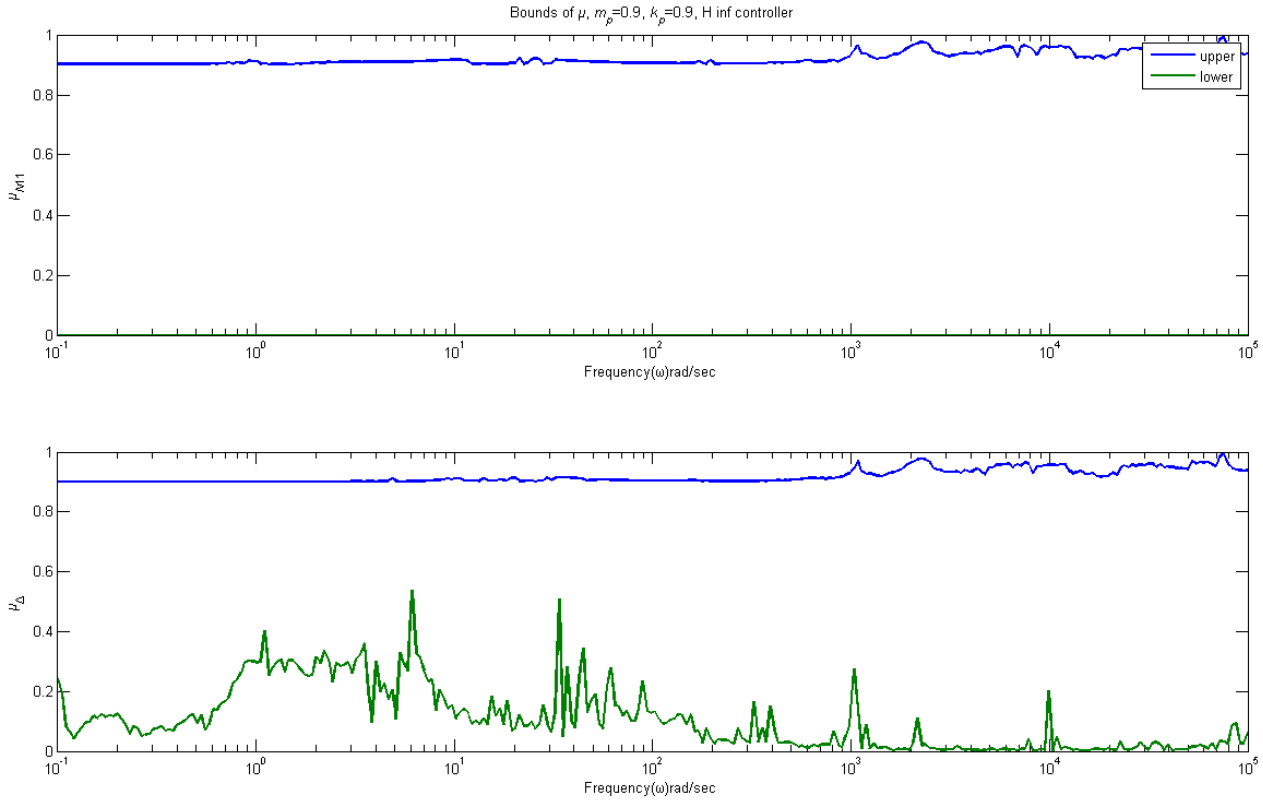

Figure 13. μ-bounds of the $H_{infinity}$ controller for $m_p = 0.9$ and $k_p = 0.9$.

3.3. Robust Synthesis: μ-Controller

A μ-controller can be designed using the previously discussed D-K iteration technique. As previously mentioned, this method approximates the μ-value and offers bounds [29–32]. To facilitate comparisons with the controller, we will apply equivalent constraints for the uncertainty. In all the simulations, we apply, at the free end of the beam, the second mechanical force of 10 N.

For the case of $m_p = 0$ and $k_p = 0.9$: this represents the stiffness matrix K to a $\pm$90% deviation from the nominal value.

As stated earlier, the necessary commands for performing this procedure in MATLAB are:

beam_u = ss(A0_u, eye(2 × nd), C, zeros(nd/2, 2 × nd));
M = iconnect;
nn = icsignal(4);
d = icsignal(8);
u = icsignal(4);
y = icsignal(4);
M.Equation{1} = equate(y, beam_u × [B0_u × u + G0_u × Wd × d]);
M.Input = [d; nn; u];
M.Output = [We × y; Wu × u; y + Wn × nn];
qbeam_w_o = M.System;
[K, qbeam_w_c_m, gam_miu] = dksyn(qbeam_w_o, m, r);
Where G0_u, B0_u and A0_u are uncertain matrix objects.

The execution of this command yields a robust controller with an order of 42. However, despite this being acknowledged in the literature, it has not been adequately addressed and is, indeed, a limitation. To our knowledge, there is not a simple approach to reducing the order, unless a laborious and tedious manual approach is employed [33–35]. Figure 14 illustrates the μ-values of the calculated controller. It is evident that the controller exhibits robustness across a wide range of frequencies [36].

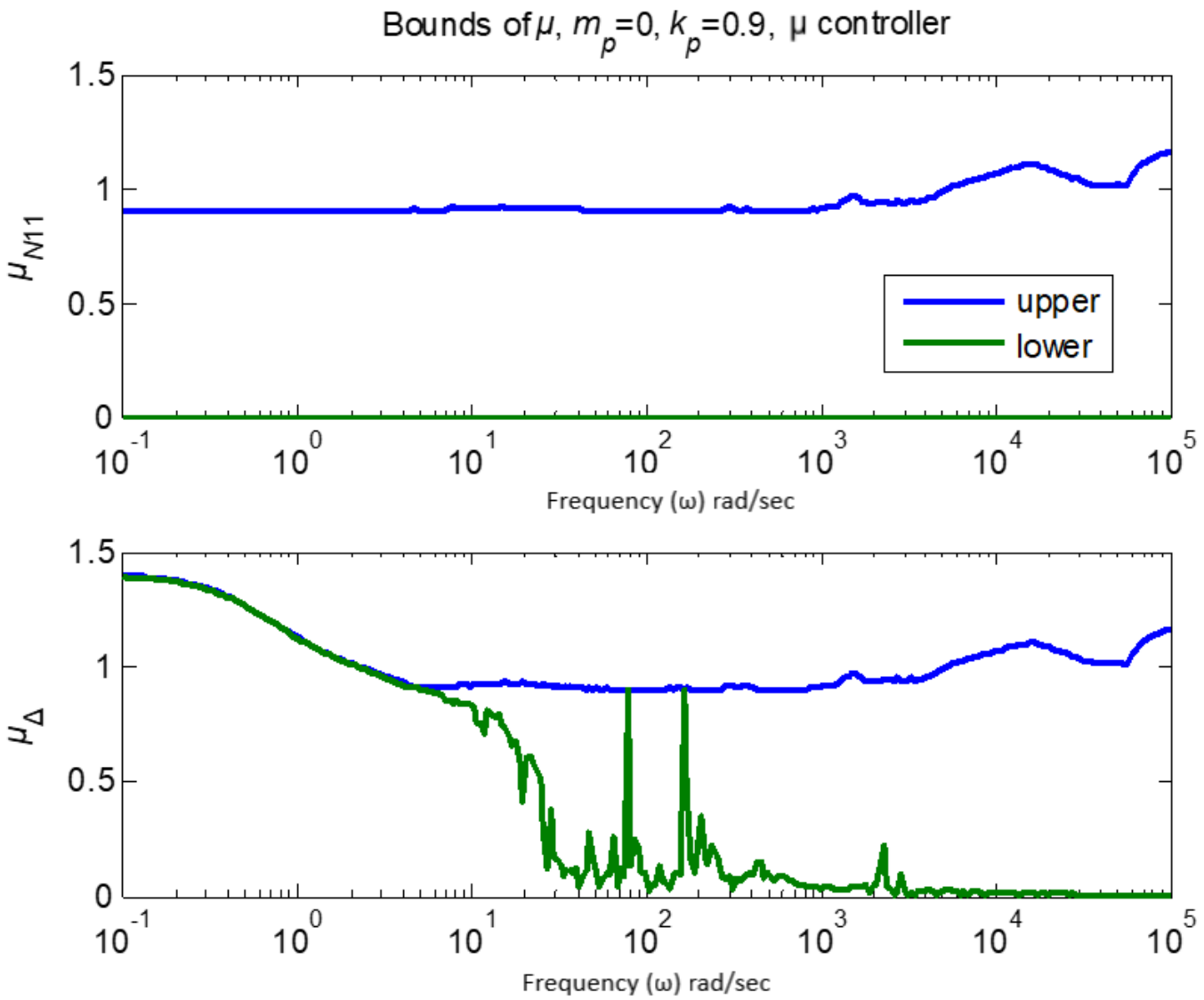

Figure 14. μ-bounds of the μ-controller for $m_p = 0$ and $k_p = 0.9$.

In Figure 15, a comparison is drawn between the performances of the μ-controller and the H∞ controller at the free end, encompassing the overall performance. It is evident that the H∞ controller outperforms the μ-controller, albeit at the expense of requiring more demanding control efforts. This observation is supported by Figure 16, which demonstrates that the H∞ controller performs more effectively at the extreme value. This variation could potentially stem from numerical challenges during the μ-controller's computation due to the plant's low condition number. The high controller order might also contribute to this disparity. For the scenario where $m_p = 0.9$ and $k_p = 0.9$: this equates to a substantial ±90% variation from the nominal values of both the mass matrix M and stiffness matrix K (Equation (16)), which means $M = 1.9 \times M_0$, $K = 1.9 \times K_0$ or $M = 0.1 \times M_0$, $K = 0.1 \times K_0$.

This paper offers novel methods for incorporating uncertainty into simulation models and damping structural oscillations using mass and stiffness matrices. A major technical novelty is the suppression of oscillations even with extremely significant modifications to the model's starting matrixes. The starting mass and stiffness vary by plus or minus 90% of the nominal value, meaning that the model varies excessively. Nevertheless, the oscillations are dampened within the piezoelectric patches' resistance limitations. This variance might be the result of model failures and modeling uncertainty.

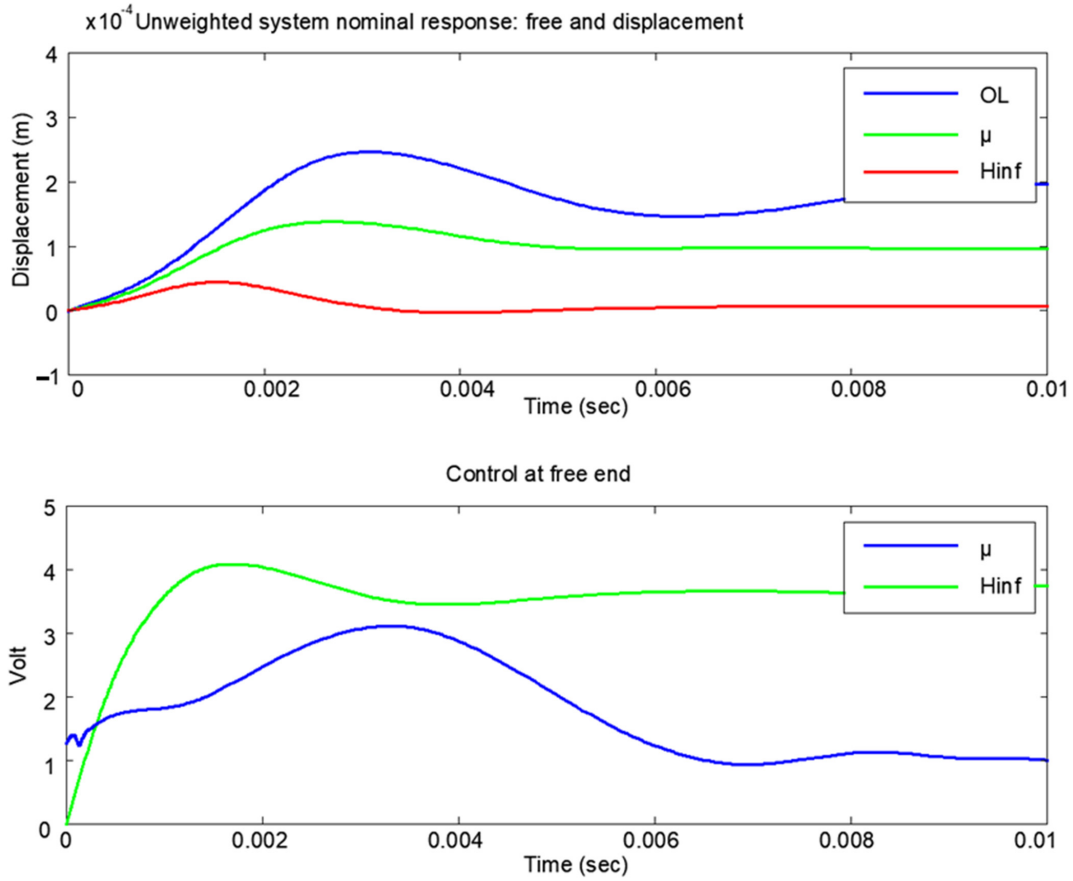

Figure 15. Free-end responses comparison for the nominal system using the μ-controller ($m_p = 0$ and $k_p = 0.9$) and H∞.

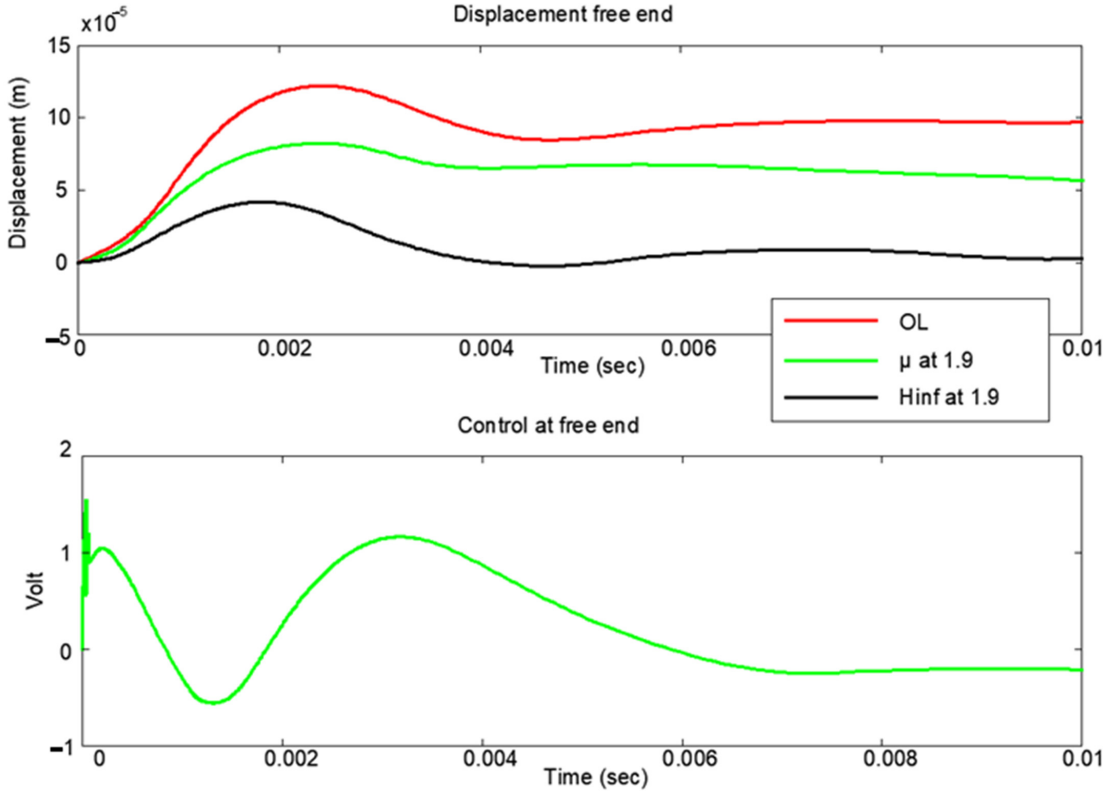

Figure 16. *Cont.*

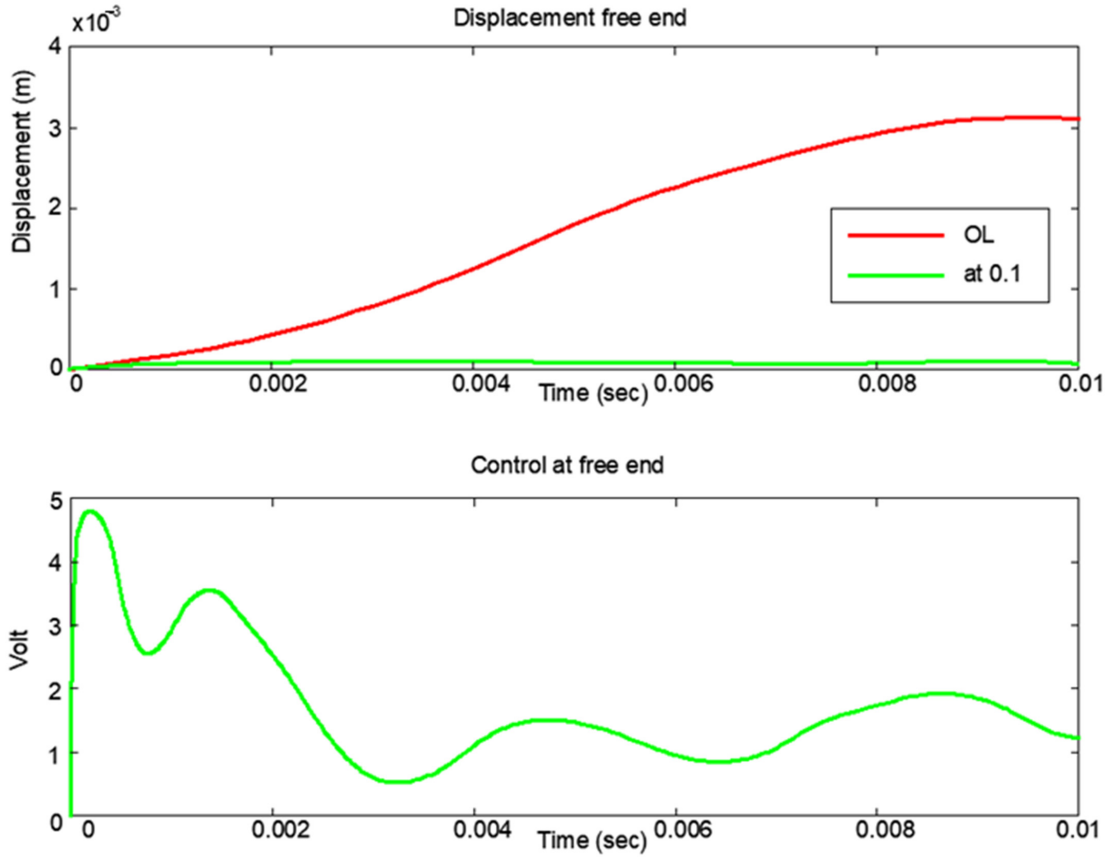

Figure 16. The displacement and control responses at the free end for the μ-controller with $m_p = 0$ and $k_p = 0.9$.

4. Discussion

A μ-analysis can improve the accuracy of the singular value function of a closed-loop system by using the structured uncertainty of the real plant. The structured singular value function is taken into consideration during the so-called D-K iteration, which may be employed in the μ-synthesis to enhance the controller. In this method, the weighting factor and controller are created through iterative steps. The joint optimization, or D-K iteration, is not convex, and global convergence is not guaranteed, yet this approach still works. The purpose of this work was to present a $H_{infinity}$-based control design approach that provided a nominal performance and dependable stability. Since it was essential for the controller, a number of nominal performance and strong stability parameters were provided. This paper's objective was to introduce a control design technique based on $H_{infinity}$ that offered a nominal performance and reliable stability. Several nominal performance and robust stability parameters were offered since it was critical for the controller design that these two types of criteria be specified. However, given that an identification procedure led to the nominal model of the inverted pendulum, this issue was more challenging. A controller that uses this model must be created in such a way that it satisfies the demands for nominal performance and robust stability for both the recognized model and the real plant. The controller design process was built around two basic elements. One situation required that high uncertainty and high-performance conditions be satisfied. Numerous design choices were offered for the selection of the strong stability and nominal performance requirements. Although the created $H_{infinity}$ controller in this study fulfilled the required high-stability criteria, it performed poorly. The created controller used D-K iteration in the μ-synthesis to guarantee a nominal and reliable performance. Control has a crucial role in structural engineering, and the use of smart materials in the sciences has been the subject of several

investigations. About these kinds of applications, there is a wealth of literature. Below are a few well-known and recent publications [11–13].

In this study, new techniques for dampening structural oscillations and adding uncertainty to simulation models using mass and stiffness matrices were provided. The suppression of oscillations was achieved even for very large changes in the initial matrices of a model, which is a great innovation in engineering. The initial mass and stiffness changed by ±90% of the nominal value, that is, the model changed too much, and despite this, the oscillations were damped within the resistance limits of the piezoelectric patches. This variation may have been due to modeling uncertainties and model failures.

By demonstrating the use of $H_{infinity}$ control and μ-analysis and synthesis in both the state space and frequency domain, the essay explored the benefits of robust control in intelligent architectures. It took into consideration a dynamic model for intelligent constructions subject to excitations caused by the wind. The design was made possible by a robust controller handling uncertainties in the dynamical system and inaccurate data observations. The effectiveness of the suggested strategies for reducing vibrations in piezoelectric smart structures was demonstrated by numerical simulations. The strategy guaranteed a thorough and unified process for creating and verifying reliable control systems. The development of intelligent structures has been made easier by $H_{infinity}$ robust controllers and μ-analysis since these take into account a dynamic system's uncertainties and inadequate data. The numerical simulation confirmed that the general techniques, provided in an instructional format, are effective at attaining good results.

5. Conclusions

This paper developed a precise model of a homogeneous smart structure with unique boundary conditions. The enhanced uncertain plant was created after modeling multiplicative uncertainty; utilizing μ-synthesis and $H_{infinity}$, an ideal robust controller was then constructed. Based on the enlarged plant made up of the nominal model and its accompanying uncertainty, a strong controller was created. For perturbed plants, the developed controllers attained robust and nominal performances, and the outcomes were compared. Two distinct methods of robust controller designs were used to manage the vibration of a smart structure with a collocated piezoelectric actuator and sensor as a generic smart structure. For both the normal and damaged laminated plates, the design of the piezoelectric active control utilizing the μ-analysis and $H_{infinity}$ control theory was investigated. The outcomes demonstrated the utility of the suggested model and methodology, and the control behavior of the beam conformed to expectations. After performing a system analysis, we evaluated the system's performance and resilient stability. The introduction of uncertainty enabled us to maintain the structure in use within predetermined uncertainty bounds. The essay explored the merits of robust control within intelligent structures by highlighting the implementation of H∞ control in both the frequency domain and state space. The following are benefits of this work: the modeling of intelligent constructs and the execution of control in oscillation suppression, results in the frequency domain as well as the time–space domain, the introduction of the uncertainties in the construction's mathematical model, an introduction to μ-analysis and μ-synthesis in smart structures. Future research will concentrate on two areas, first applying these control strategies to actual intelligent structures in an experimental setting and next employing different control methods for structural noise and vibration suppression.

Author Contributions: G.E.S.: methodology; A.M. and M.P.: software, writing—review, and editing; N.V.: validation; M.P.: formal analysis; A.P.: investigation, software. All authors have read and agreed to the published version of the manuscript.

Funding: This research received no external funding.

Data Availability Statement: The data presented in this study are available on request from the corresponding author.

Acknowledgments: The authors are grateful for the support from Hellenic Mediterranean University and the Technical University of Crete.

Conflicts of Interest: The authors declare no conflict of interest.

References

1. Tzou, H.S.; Gabbert, U. Structronics—A New Discipline and Its Challenging Issues. *Fortschr.-Berichte VDI Smart Mech. Syst. Adapt. Reihe* **1997**, *11*, 245–250.
2. Guran, A.; Tzou, H.-S.; Anderson, G.L.; Natori, M.; Gabbert, U.; Tani, J.; Breitbach, E. *Structronic Systems: Smart Structures, Devices and Systems*; World Scientific: Singapore, 1998; Volume 4, ISBN 978-981-02-2652-7.
3. Tzou, H.S.; Anderson, G.L. *Intelligent Structural Systems*; Springer: Dordrecht, The Netherlands; Boston, MA, USA; London, UK, 1992; ISBN 978-94-017-1903-2.
4. Gabbert, U.; Tzou, H.S. IUTAM Symposium on Smart Structures and Structronic Systems. In Proceedings of the IUTAM Symposium, Magdeburg, Germany, 26–29 September 2000; Kluwer: Dordrecht, The Netherlands; Boston, MA, USA; London, UK, 2001.
5. Tzou, H.S.; Natori, M.C. *Piezoelectric Materials and Continua*; Elsevier: Oxford, UK, 2001; pp. 1011–1018. ISBN 978-0-12-227085-7.
6. Cady, W.G. *Piezoelectricity: An Introduction to the Theory and Applications of Electromechanical Phenomena in Crystals*; Dover Publication: New York, NY, USA, 1964.
7. Tzou, H.S.; Bao, Y. A Theory on Anisotropic Piezothermoelastic Shell Laminates with Sensor/Actuator Applications. *J. Sound Vib.* **1995**, *184*, 453–473. [CrossRef]
8. Das Mahapatra, S.; Mohapatra, P.C.; Aria, A.I.; Christie, G.; Mishra, Y.K.; Hofmann, S.; Thakur, V.K. Piezoelectric Materials for Energy Harvesting and Sensing Applications: Roadmap for Future Smart Materials. *Adv. Sci.* **2021**, *8*, 2100864. [CrossRef] [PubMed]
9. Bahl, S.; Nagar, H.; Singh, I.; Sehgal, S. Smart materials types, properties and applications: A review. *Mater. Today Proc.* **2020**, *28*, 1302–1306. [CrossRef]
10. Vidakis, N.; Petousis, M.; Mountakis, N.; Papadakis, V.; Moutsopoulou, A. Mechanical Strength Predictability of Full Factorial, Taguchi, and Box Behnken Designs: Optimization of Thermal Settings and Cellulose Nanofibers Content in PA12 for MEX AM. *J. Mech. Behav. Biomed. Mater.* **2023**, *142*, 105846. [CrossRef] [PubMed]
11. Zaszczyńska, A.; Gradys, A.; Sajkiewicz, P. Progress in the applications of smart piezoelectric materials for medical devices. *Polymers* **2020**, *12*, 2754. [CrossRef]
12. Koc, B.; Delibas, B. Actuator. U.S. Patent 11,336,208, 17 May 2022.
13. Yu, J.; Yang, X.; Sun, Q. Piezo/tribotronics toward smart flexible sensors. *Adv. Intell. Syst.* **2020**, *2*, 1900175. [CrossRef]
14. Cen, S.; Soh, A.-K.; Long, Y.-Q.; Yao, Z.-H. A New 4-Node Quadrilateral FE Model with Variable Electrical Degrees of Freedom for the Analysis of Piezoelectric Laminated Composite Plates. *Compos. Struct.* **2002**, *58*, 583–599. [CrossRef]
15. Yang, S.M.; Lee, Y.J. Optimization of Noncollocated Sensor/Actuator Location and Feedback Gain in Control Systems. *Smart Mater. Struct.* **1993**, *2*, 96. [CrossRef]
16. Schwenzer, M.; Ay, M.; Bergs, T.; Abel, D. Review on model predictive control: An engineering perspective. *Int. J. Adv. Manuf. Technol.* **2021**, *117*, 1327–1349. [CrossRef]
17. Garcia-Sanz, M. Control Co-Design: An engineering game changer. *Adv. Control Appl.* **2019**, *1*, e18. [CrossRef]
18. Moutsopoulou, A.; Stavroulakis, G.E.; Petousis, M.; Vidakis, N.; Pouliezos, A. Smart Structures Innovations Using Robust Control Methods. *Appl. Mech.* **2023**, *4*, 856–869. [CrossRef]
19. Ramesh Kumar, K.; Narayanan, S. Active Vibration Control of Beams with Optimal Placement of Piezoelectric Sensor/Actuator Pairs. *Smart Mater. Struct.* **2008**, *17*, 55008. [CrossRef]
20. Hanagud, S.; Obal, M.W.; Calise, A.J. Optimal Vibration Control by the Use of Piezoceramic Sensors and Actuators. *J. Guid. Control. Dyn.* **1992**, *15*, 1199–1206. [CrossRef]
21. Song, G.; Sethi, V.; Li, H.-N. Vibration Control of Civil Structures Using Piezoceramic Smart Materials: A Review. *Eng. Struct.* **2006**, *28*, 1513–1524. [CrossRef]
22. Bandyopadhyay, B.; Manjunath, T.C.; Umapathy, M. *Modeling, Control and Implementation of Smart Structures A FEM-State Space Approach*; Springer: Berlin/Heidelberg, Germany, 2007; ISBN 978-3-540-48393-9.
23. Miara, B.; Stavroulakis, G.E.; Valente, V. Topics on Mathematics for Smart Systems. In Proceedings of the European Conference, Rome, Italy, 26–28 July 2022; World Scientific Publishing Co., Inc.: Singapore, 2022.
24. Moutsopoulou, A.; Stavroulakis, G.E.; Pouliezos, A.; Petousis, M.; Vidakis, N. Robust Control and Active Vibration Suppression in Dynamics of Smart Systems. *Inventions* **2023**, *8*, 47. [CrossRef]
25. Zhang, N.; Kirpitchenko, I. Modelling Dynamics of A Continuous Structure with a Piezoelectric Sensoractuator for Passive Structural Control. *J. Sound Vib.* **2002**, *249*, 251–261. [CrossRef]
26. Zhang, X.; Shao, C.; Li, S.; Xu, D.; Erdman, A.G. Robust H∞ Vibration Control for Flexible Linkage Mechanism Systems with Piezoelectric Sensors and Actuators. *J. Sound Vib.* **2001**, *243*, 145–155. [CrossRef]
27. Packard, A.; Doyle, J.; Balas, G. Linear, Multivariable Robust Control with a μ Perspective. *J. Dyn. Syst. Meas. Control* **1993**, *115*, 426–438. [CrossRef]

28. Stavroulakis, G.E.; Foutsitzi, G.; Hadjigeorgiou, E.; Marinova, D.; Baniotopoulos, C.C. Design and Robust Optimal Control of Smart Beams with Application on Vibrations Suppression. *Adv. Eng. Softw.* **2005**, *36*, 806–813. [CrossRef]
29. Kimura, H. Robust Stabilizability for a Class of Transfer Functions. *IEEE Trans. Autom. Control* **1984**, *29*, 788–793. [CrossRef]
30. Burke, J.V.; Henrion, D.; Lewis, A.S.; Overton, M.L. Stabilization via Nonsmooth, Nonconvex Optimization. *IEEE Trans. Autom. Control* **2006**, *51*, 1760–1769. [CrossRef]
31. Doyle, J.; Glover, K.; Khargonekar, P.; Francis, B. State-Space Solutions to Standard H2 and H∞ Control Problems. In Proceedings of the 1988 American Control Conference, Atlanta, GA, USA, 15–17 June 1988; pp. 1691–1696.
32. Francis, B.A. *A Course in H∞ Control Theory*; Springer: Berlin/Heidelberg, Germany, 1987; ISBN 978-3-540-17069-3.
33. Turchenko, V.A.; Trukhanov, S.V.; Kostishin, V.G.; Damay, F.; Porcher, F.; Klygach, D.S.; Vakhitov, M.G.; Lyakhov, D.; Michels, D.; Bozzo, B.; et al. Features of Structure, Magnetic State and Electrodynamic Performance of SrFe12−xInxO19. *Sci. Rep.* **2021**, *11*, 18342. [CrossRef] [PubMed]
34. Kwakernaak, H. Robust Control and H∞-Optimization—Tutorial Paper. *Automatica* **1993**, *29*, 255–273. [CrossRef]
35. Chandrashekhara, K.; Varadarajan, S. Adaptive Shape Control of Composite Beams with Piezoelectric Actuators. *J. Intell. Mater. Syst. Struct.* **1997**, *8*, 112–124. [CrossRef]
36. Zames, G.; Francis, B. Feedback, Minimax Sensitivity, and Optimal Robustness. *IEEE Trans. Autom. Control* **1983**, *28*, 585–601. [CrossRef]